EDSU Journal of Engineering and Technology (EDSUJET) Vol. 2 (1), pp. 173 – 190. 2026
ISSN (Print):3121 – 8725 eISSN (Online): 3121 – 8597

Coupled Thermal-Structural Loading and Performance Analysis of a Connecting Rod in a Diesel Engine

Stephen Olusegun Adediran[a],* and Festus Oamen Isaac[b]

[a]Faculty of Engineering, Department of Mechanical Engineering, Edo State University Iyamho. Edo State, Nigeria. stephenbelt2003@gmail.com
[b]Faculty of Engineering, Department of Mechanical Engineering, Edo State University Iyamho. Edo State, Nigeria. isaac.oamen@edouniversity.edu.ng
*Corresponding author email: stephenbelt2003@gmail.com

Received: 28th November 2025, Accepted: 7th February 2026, Published: 31 March 2026

KEYWORDS

ANSYS 2024 R1
AA356.0-T6
Al7039/Cu/SiC
Al7050-T7451;
Finite Element Method
Thermal-Structural Analysis.

ABSTRACT

The purpose of this research is to evaluate the coupled thermal–structural response of a diesel engine connecting rod and to identify the most efficient material capable of maintaining structural integrity under realistic operating temperatures and mechanical loads. A coupled thermal–structural finite element analysis was conducted using ANSYS 2024 R1, in which a three-dimensional connecting rod model was subjected to combustion-induced thermal loads and mechanical loads arising from gas pressure and inertia forces. Three aluminum-based materials—AA356.0-T6, Al7039/Cu/SiC metal–matrix composite, and Al7050-T7451—were investigated to assess their thermo-mechanical performances. The result indicates that AA356.0-T6 and Al7039/Cu/SiC experienced excessive thermal deformations of 27.719 mm and 29.778 mm, respectively, with equivalent stresses exceeding 11,000 MPa, reflecting poor stability under coupled loading. In contrast, Al7050-T7451 exhibited significantly lower deformation of 2.9211 mm and a maximum stress of 502.62 MPa. The major findings demonstrate that Al7050-T7451 possesses superior resistance to thermal expansion and stress concentration compared with the other materials evaluated. The major conclusion drawn from this study is that Al7050-T7451 is the most suitable material for diesel engine connecting rod applications, offering enhanced thermo-mechanical stability, improved reliability, and reduced risk of failure under elevated temperature and pressure conditions.

1. INTRODUCTION

Automotive sector is a very fast growing and developing sector which required cost reduction and quality improvement. Hence, the need for constant innovations for optimum design in this

sector is highly recommended. Research and Development projects and academic research are made frequently on this topic (Andreas, 2024). Engine is one of the basic components of vehicles, thereby making innovations in engines to have critical influence on emission and performance of automobile directly. New designs for engine components are generally made to decrease weight, reduce cost and improved performance by enhancing desired operating conditions. The most widely used techniques in light-weight studies are topology, topography, size, shape optimization, and metaheuristic algorithms. The optimum design on sizing, shape and topology optimization had contributed to cost, material and time savings. The focus is on shape optimization, which aims to minimize the weight of the vehicle component while ensuring that stress constraints are met. (Yildiz1a and Yıldız,1b 2024).

The connecting rod is a basic mechanical component in internal combustion engines of automobiles and stationary engines. It plays a vital role in transmitting the piston's reciprocating motion to the rotary motion of the crankshaft (Maher, 2024)

Diesel engines, in particular, operate under harsh conditions, with high pressures, temperatures, strains and stresses. This called for an optimized connecting rod design to ensure reliability, efficiency, and optimum performance, any failure of the connecting rod will certainly cause catastrophic damage to the engine (Anand and Raghukumar, 2022).

The connecting rod, sometimes also referred to as the con rod is a crucial component of internal combustion engines that has undergone significant transformations since its inception. Due to its function, the connecting rod is exposed to extremely strong forces in form of tension, pressure and bending or buckling, especially when increasing performance as part of engine improvement (Autodoc, 2023)

This is why different types of connecting rods are available, each designed for a specific area of application and specific loads (Gangarkar and Prashant, 2024). The connecting rod transfers the energy released during the combustion process from the piston to the engine’s crankshaft. For this reason, it is connected to both components and mounted so that it can move. Nowadays, connecting rods in modern ICEs have to meet a wide variety of standards. In order for the combustion engine to operate efficiently, they must be both strong and lightweight. This is why they are constructed with special materials depending on the type of internal combustion engine, which means that the cost of the component can differ depending on the design (Gangarkar and Prashant, 2024).

The result from advance investigations using FEM showed that during engine operations with maximum power, the high stress zones are always located in crack origins. Obtained results indicated that the bolt tightening torque has a significant influence on maximum value of stress at crack origin. Based on results of performed investigations it was concluded that the main reason of the connecting rod's failure was a high stress levels in zones near the bolt hole caused by high pretension of bolts (Zhu, et al, 2017).

Failure of connecting rods is mainly caused by fatigue and factors which results from improper material selection, poor design or fabrication defects (Griza, et al 2009). The majority of damages have been reported to take place at some parts of connecting rod such as a small end of the connecting rod, crank pin, roller bearing and connecting rod bolt (Arso, et al, 2024; Zhu,

et al, 2017; Gautam, et al, 2021).

The optimization aims is to minimize the structural and thermal stresses experienced by the connecting rod under both compressive loads from maximum engine output and bending loads caused by the inertia force during maximum engine power with a focused on reducing its weight. (Gangarkar and Karajagi, 2024). The use of FEM in ANSYS would enhances the identification of the regions of the connecting rod with less von Mises stress to allow for the reduction of weight at the regions (Mohamed *et al,* 2014), increasing the radius near the cap bolts would strengthen the region to withstand fatigue failure that normally occurs in the region and as a result increased the durability of the connecting rod. Reduction in weight and increase in the strength invariably reduce the production and running cost of the entire engine with lesser fuel consumption (Chirinda and Matope, 2020).
The aim of this study is to select the best material for connecting rod of a diesel engine through the coupled thermal-structural analysis using finite element method in ANSYS. The other specific objectives are:

1. To carry out the design of connecting rod components using **relevant** equations
2. To model connecting rod in SOLIDWORKS 2023
3. To import the models into ANSYS 2024R1 commercial software for simulation
4. To carry out the thermal-structural and performance analysis of thermal stresses by material variations of the model to reduce deformation and thermal stresses.
5. To select the most efficient connecting rod by using the best material with less deformation and von-Mises stress during coupled thermal-structural simulation.

2. MATERIALS AND METHODS

2.1 Material Selection

The materials chosen for this study were AA356.0-T6, Al7050-T7451 and Aluminum Metal Matrix Composites Al7039/Cu/SiC for its better thermal conductivity than aluminum alloys. Tables 1 shows the Chemical composition of the connecting rod materials while Table 2 shows the Mechanical, Physical and Thermal properties of the selected materials for the connecting rod.
The cross-section of connecting rod can be two types I-beam & H-beam or the combination of two known as X-Beam. H-Beam can take care of large stress and anxiety without flexing so used in high power engines. I -beam manage high-pressure, light and strong. In a study H-beam profile is better than I-beam profile because it has more stability – up to 43.1% and von Mises stresses are also less up to 12.3% (average – 15.7%). But I-beam is being used more as it is easier and less expensive to manufacture it, (Godara, et al, 2022); hence I-beam is used for this study.

The Design Input parameters were obtained from the WP10.336 Weichai diesel engine, Weichai Diesel Engine consists of six cylinders pistons. The details are as tabulated below (Weichai Power Company Limited, 2017)

2.2 Methodology Flowchart

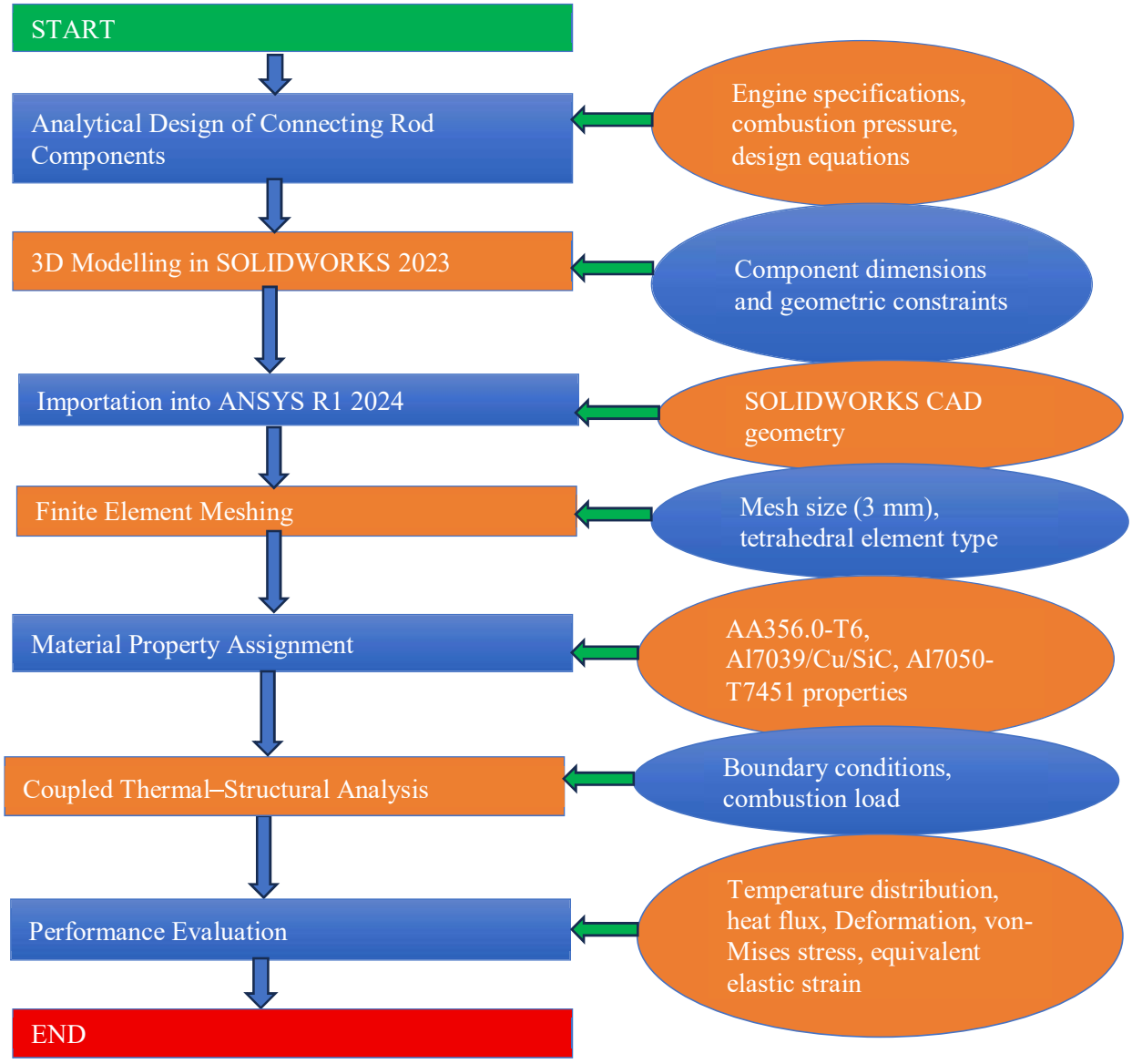

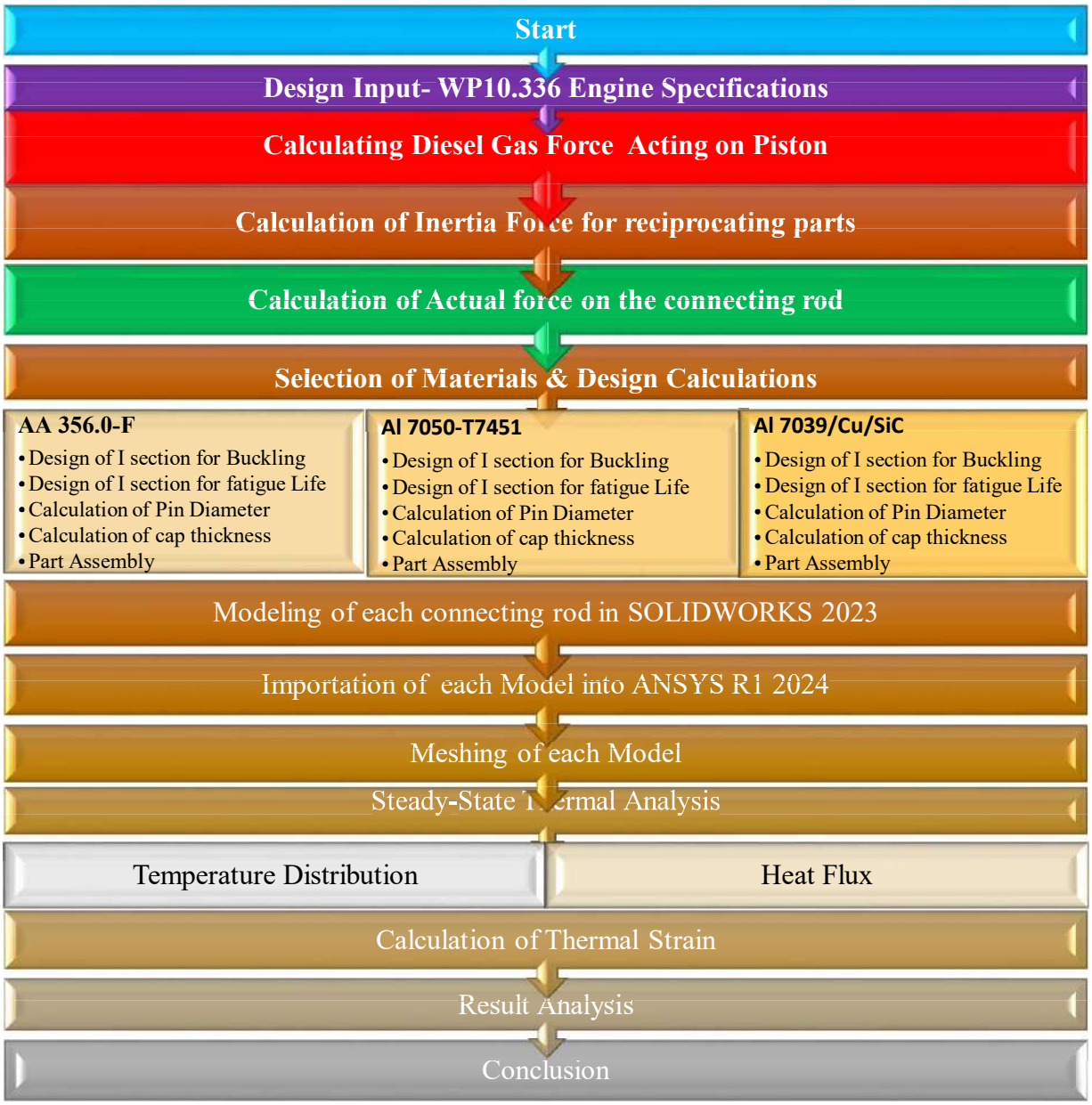
Start
Design Input- WP10.336 Engine Specifications
Calculating Diesel Gas Force Acting on Piston
Calculation of Inertia Force for reciprocating parts
Calculation of Actual force on the connecting rod
Selection of Materials & Design Calculations
AA 356.0-F
• Design of I section for Buckling
• Design of I section for fatigue Life
• Calculation of Pin Diameter
• Calculation of cap thickness
• Part Assembly
Al 7050-T7451
• Design of I section for Buckling
• Design of I section for fatigue Life
• Calculation of Pin Diameter
• Calculation of cap thickness
• Part Assembly
Al 7039/Cu/SiC
• Design of I section for Buckling
• Design of I section for fatigue Life
• Calculation of Pin Diameter
• Calculation of cap thickness
• Part Assembly
Modeling of each connecting rod in SOLIDWORKS 2023
Importation of each Model into ANSYS R1 2024
Meshing of each Model
Steady-State Thermal Analysis
Temperature Distribution
Heat Flux
Calculation of Thermal Strain
Result Analysis
Conclusion

Table 1: Chemical composition of the connecting rod materials

Element	AA 356.0-T6	Al7050-T7451	Al 7039/Cu/SiC
Iron, Fe (%)	0.6	0.15	0.35
Chromium,Cr (%)		0.04	0.1
Manganese,Mn(%)	0.35	0.1	0.03
Zinc, Zn(%)	0.35	5.7 – 6.7	0.05
Silicon, Si(%)	7.5	0.12	0.84
Silicon Carbide(%)			15
Al	90.1	87.3 – 90.3	69.22
Titanium, Ti	0.25	0.06	0.03
Zr		0.08 – 0.15	
Magnesium, Mg	0.45	1.9 – 2.6	0.02
Copper, Cu	0.25	2 – 2.6	12
Others	0.15	0.15	

(Source: ASM, 2019; Aerospace Metal, 2023; Teferi, 2025; Smith Metal 2023; Teng, et al 2023).

Table 2: Mechanical, Physical and Thermal properties of the connecting rod material

Element	AA 356.0-T6	Al7050-T7451	Al 7039/Cu/SiC
Tensile strength (MPa)	131MPa	524MPa	610MPA
Compressive Yield strength	90MPa	434MPa	400MPa
Shear modulus (typical for steel)	27.2GPa	26.9GPa	26.9GPa
Elastic modulus	72.4GPa	72GPa	100GPa
Poisson's ratio	0.33	0.33	0.30
Density(g/cm^3)	2.6	2.83	2.73
Thermal expansion co-efficient (µm/m°C)	21.4	23.6	18.55
Thermal conductivity (typical steel) (W/Mk)	150	157	169.6
Specific Heat(J/kg.K)	963	860	745.8

(Source: ASM, 2019; Aerospace Metal, 2023; Teferi, 2025; Smith Metal, 2023; Teng, et al 2023).

2.3 Design Calculations of Connecting Rods using the Selected Materials

2.3.1 Pressure for WEICHAI WP10.336 Diesel Engine

Max. speed = 1900rpm, Maximum combustion pressure =7.58MPa, Combustion Gas Temperature 1001K from weichai engine data.
All equations were obtained from Khurmi, R. and Gupta, J.K., (2005) A Textbook of Machine Design Text of Machine Design. Eurasia Publishing House (Pvt.) Ltd., New Delhi.]

2.3.2 Calculation of Force due Gas Pressure

$$F_p = P * A = P * \frac{\pi D^2}{4} \quad (1)$$

Table 3: Engine specifications for WP10.33 diesel engine

SN	Parameter	Symbol	Value	Unit
1	Engine Model	WP10.336		
2	Engine Type	Turbocharged-Intercool	6	Cylinders
3	Engine Capacity	V_s	9726	ml
4	Bore Diameter	d	126	mm
5	Stroke	s	130	mm
6	Con Rod Length	l	219	mm
7	Rated Speed	N	1900	rpm
8	Rated Power		247	Kw
9	Mass of connecting rod	Mc	3.708	Kg
10	Mass of Piston Assy & Pin	Mp	7.188	Kg
11	Max Combustion Temperature		1001	K
12	Max Combustion Pressure	Pg	7.58	N/mm^2
13	Max torque		1500	Nm

2.3.3 Calculation of force due to Inertia

$$Inertia\ Force, F_I = m \cdot \omega^2 \cdot r\left(cos\,\theta + \frac{cos\,2\theta}{n}\right) \quad (2)$$

$$n = \frac{l}{r} = \frac{2 \times stroke}{stroke/_2} \quad (3)$$

Total Force acting $F = F_p \pm F_I$ (4)

Where,

F_P = force acting on the piston

F_I = force of inertia

$W_B = F \times F.S$, where F.S is safety factor and W_B = buckling force (5)

$$W_B = \frac{\sigma_c \,.\, A}{1 + a\left(\frac{L}{K_{xx}}\right)^2} \quad (6)$$

$A = 2\,(4\,t \times t) + 3\,t \times t = 11\,t^2$; where t is the thickness web thickness (7)

Moment of inertia of the section about X-axis: I_{xx}

$$I_{xx} = \frac{1}{12}[4t \times (5t)^3 - 3t(3t)^3] = \frac{419}{12}t^4 \quad (8)$$

Moment of inertia of the section about Y-axis: I_{yy}

$$I_{yy} = \left[2 \times \frac{1}{12}t \times (4t)^3 + \frac{1}{12}(3t)t^3\right] = \frac{131}{12}t^4 \quad (9)$$

2.3.4 Calculation of the radius of gyration

The radius of gyration about X- axis is

$$K_{xx} = \sqrt{\frac{I_{xx}}{A}} = \sqrt{\frac{419}{12}t^4 \times \frac{1}{11\,t^2}} = 1.7816t \quad (10)$$

2.3.5 Heat Transfer-Coefficient

The heat-transfer-coefficient under piston-crown and crankcase is calculated using equation (Puran & Deb, 2015) expressed as:

$$h_{oil} = 900\left(\frac{N}{4600}\right)^{0.35} \quad (11)$$

3.0 RESULTS AND DISCUSSIONS

3.1 Calculation of Force due Gas Pressure

$F_p = 7.58 * \frac{\pi D^2}{4} = 7.58 * \frac{\pi(126)^2}{4} = 94527.1328N$ from equation (1)

3.1.1 Calculation of force due to Inertia

The maximum gas load occurs shortly after the dead centre position at θ = 3.3°, Cos3.3 = 0.9983≅ 1; from equations (2 and 3)

$$F_I = 1.394 \times \left(\frac{2\pi \times 1900}{60}\right)^2 \times 0.065 \times \left(1 + \frac{1}{4}\right) = 4483.8449$$

3.1.2 Total Force acting F ; from equation (4)

$$F = 94527.1328N - 4483.8449 = 90043.28794N$$

3.1.3 Buckling Load

Now let us find the dimensions of this I-section. Since the connecting rod is designed by taking the force on the connecting rod (F_P) equal to the maximum force on the piston (F_L) due to gas pressure, therefore, we know that the connecting rod is designed for buckling about X-axis (i.e. in the plane of motion of the connecting rod) assuming both ends hinged. Taking 2 as presumed safety factor, therefore the buckling load,

$W_B = F \times 2 = 180086.27588$ from equation (5)

3.1.4 Ratio of moment of inertia: equation (8) / equation (9)

$= \frac{I_{xx}}{I_{yy}} = 3.2$

Since the ratio of the moment of inertia of $I_{xx}\ to\ I_{yy}\ is\ 3.2\ the$ design shape satisfied the buckling condition.

3.2 Design Calculation for the Connecting Rod using Al7050-T7451 Aluminium Alloy

$\sigma_c = 434MPa;\ a = \frac{1}{9000};\ L = l = 219mm, ie\ connecting\ rod\ hinged\ at\ both\ ends = 219mm\ from\ engine\ manual$

3.2.1 Thickness of the I-section web, t; from equations 5, 6, & 7

$$180086.27588 = \frac{434 \times 10^6 \times 11\ t^2}{1 + \frac{1}{9000} \times \left(\frac{0.219}{1.7816t}\right)^2} = \frac{4774 \times 10^6\ t^4}{t^2 + 1.678902 \times 10^{-6}}$$

$$180086.27588\ (t^2 + 1.678902 \times 10^{-6}) = 4774 \times 10^6\ t^4$$

$$180086.27588\ t^2 + 0.3023477 = 4774 \times 10^6\ t^4$$

$$-4774 \times 10^6\ t^4 + 180086.27588\ t^2 + 0.33244 = 0$$

$$t = -6.2838 \times 10^{-3}m;\ 6.2838 \times 10^{-3}m; (1.328 \times 10^{-3}m)i; (-1.328 \times 10^{-3}m)i$$

The solution gave two real roots and two complex roots, hence the selection of positive real root

$$\therefore t = 6.28mm \cong 6mm$$
$$H = 5t = 5 \times 6 = 30mm$$
$$B = 4t = 4 \times = 24mm$$
$$H_1 = 1.25 * H = 1.25 * \ 30 = 37.5 \cong 38mm$$
$$H_2 = 0.9 * H = 0.9 * \ 30 = 27mm$$

The same calculation was carried out for the AA356.0-T6 and Al7039/Cu/SiC and the resulted dimensions of the connecting rods are tabulated below:

Table 4: Dimensions of designed connecting rod for the selected materials

Items Descriptions	**Connecting rod Dimensions for selected Materials(mm)**		
	AA 356.0-F	**Al7050-T7451**	**Al 7039/Cu/SiC**
Thickness of connecting rod (*t*)	13	6	7
Height of the section (H)	65	30	35
Width of the section (B)	52	24	28
Height at the Big End (H1)	81	38	44
Height at the small end (H2)	59	27	32
Inner diameter of the Small End(dp)	60	60	60
Outer diameter of the Small End(Dp)	86	86	86
Inner diameter of the Big End (dc)	88	88	88
Outer diameter of the Big End(Dc)	132	120	120
Thickness of the big end cap (t_c)	29	13	13

4.0 RESULTS AND DISCUSSIONS

4.1 Thermal-Structural Analysis Results

AA356.0-T6 was Meshed into 107150 nodes and 60640 elements tetrahedron element type and element size of 3mm. Boundary conditions: Big end was fixed and 7.58MPa pressure was applied to the small end. The same conditions were applied to the three models and generated the simulation results pasted below.

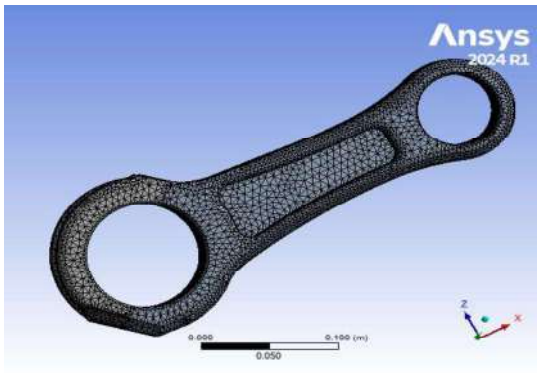

Figure 1: Mesh

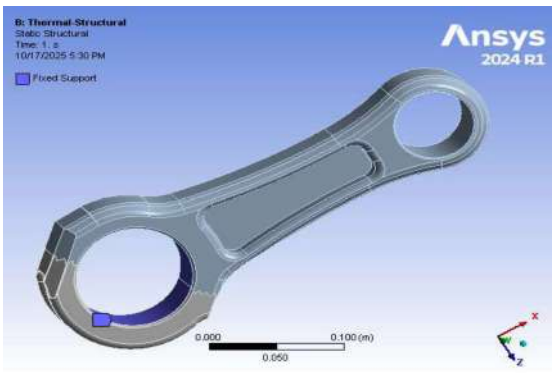

Figure 2: Boundary Conditions

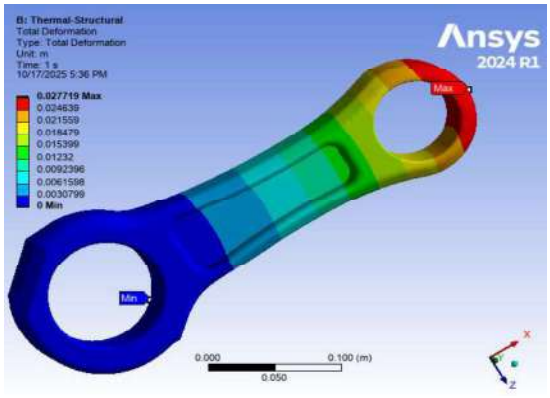

Figure 3: Total Deformation

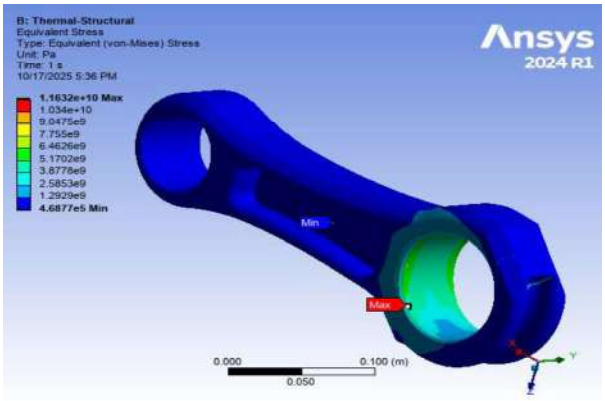

Figure 4: Von Mises Stress

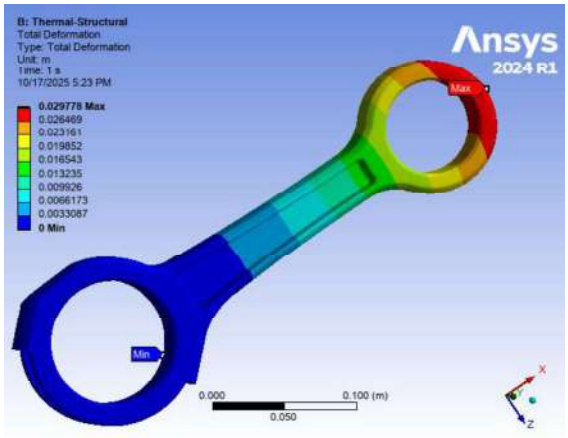

Figure 5: Total Deformation

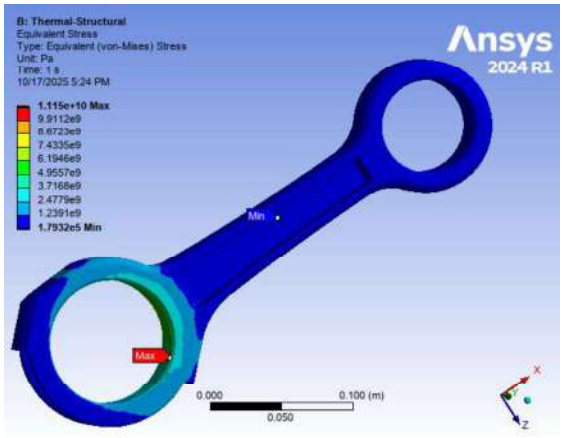

Figure 6: Von Mises Stress

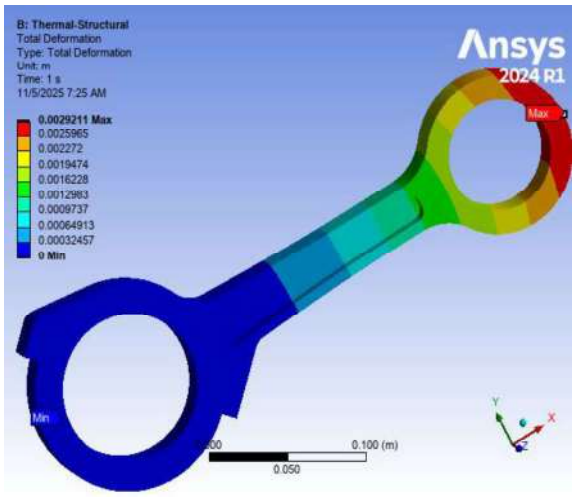

Figure 7: Von Mises Stress

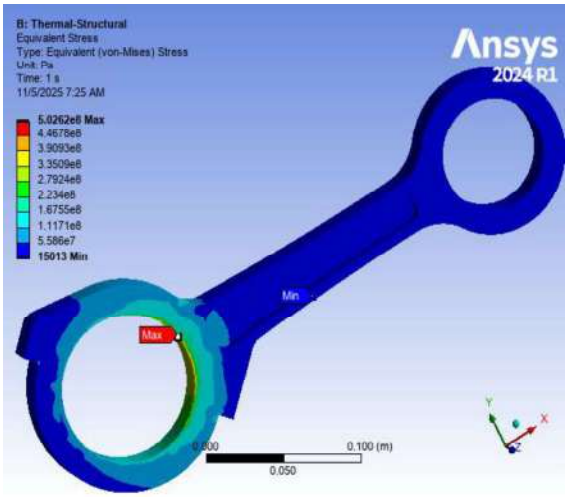

Figure 8: Total Deformation

Table 5: Results of Thermal-Structural Analysis from Figures 3 - 8

Model		Total Deformation(mm)	Von-Mises Stress (MPa)
AA356.0-T6	Max	27.719	11632
	Min	0	0.46877
Al7039/Cu/SiC	Max	29.778	11150
	Min	0	0.17932
AlA7050-T7451	Max	2.9211	502.62
	Min	0	0.15013

Figures 1 – 4 for AA356.0-T6 Thermal-Structural Simulation Results
Figures 5 & 6 for Al7039/Cu/SiC Thermal-Structural Simulation Results
Figures 7 & 8 for AlA7050-T7451 Thermal-Structural Simulation Results

Table 5 presents a comparative summary of the coupled thermal–structural analysis results (Figures 3 – 8) for the diesel engine connecting rod using three aluminum-based materials: AA356.0-T6, Al7039/Cu/SiC, and Al7050-T7451. The performance evaluation was based on total deformation and von Mises stress, which are critical indicators of dimensional stability and structural integrity under combined thermal and mechanical loading.

The AA356.0-T6 connecting rod recorded a maximum total deformation of 27.719 mm and a peak von Mises stress of 11,632 MPa (Figures 3 & 4). These high values indicate significant thermo-elastic expansion and severe stress concentration, suggesting limited resistance to coupled thermal–mechanical loads. Such behaviour implies a high likelihood of distortion and premature failure when subjected to diesel engine operating conditions.
Similarly, the Al7039/Cu/SiC composite exhibited the highest total deformation of 29.778 mm and a maximum von Mises stress of 11,150 MPa (Figures 5 & 6). Despite the presence of SiC reinforcement, the material demonstrated poor dimensional stability and excessive stress levels, indicating that the composite was unable to effectively mitigate thermally induced stresses in the connecting rod configuration.

In contrast, Al7050-T7451 showed a substantially lower maximum deformation of 2.9211 mm and a peak von Mises stress of 502.62 MPa (Figure 7 & 8). These results reflect superior stiffness, high strength, and enhanced resistance to thermal expansion. The significantly reduced stress concentration further confirms the material's ability to withstand combined loading without yielding.

Overall, the results in Table 5 clearly established Al7050-T7451 as the most thermo-mechanically efficient material among those investigated. Its low deformation and stress values demonstrate excellent structural stability and make it the most suitable candidate for connecting rod applications in high-temperature diesel engine environments. Figures 9 and 10 displayed the comparative charts.

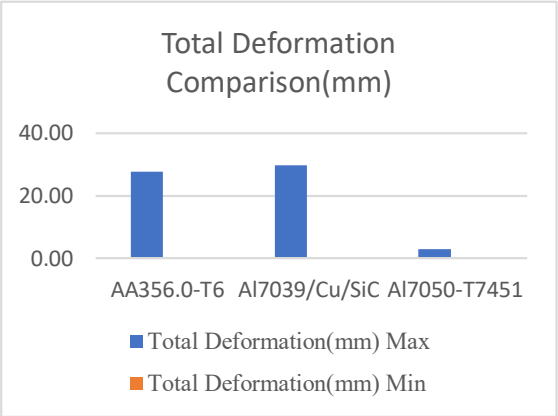

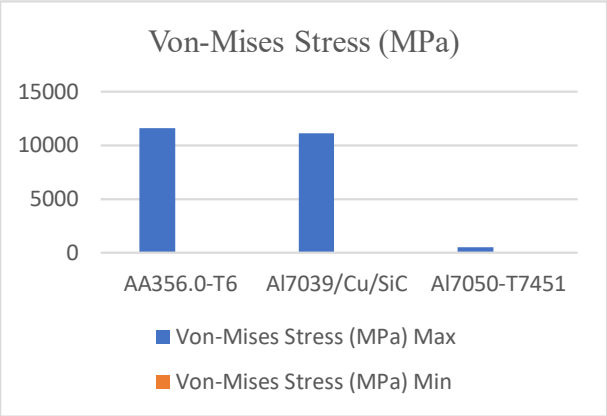

Figure 9: Total Deformation Comparison

Figure 10: von-Mises Stress Comparison

4.2 Overview Weight of the three Models Data

Table 6 Weight of Each Model Obtained from SOLIDWORKS

Model	Weight(kg)
AA356.0-T6	2.0716
Al7039/Cu/SiC	0.8718
AlA7050-T7451	0.7214

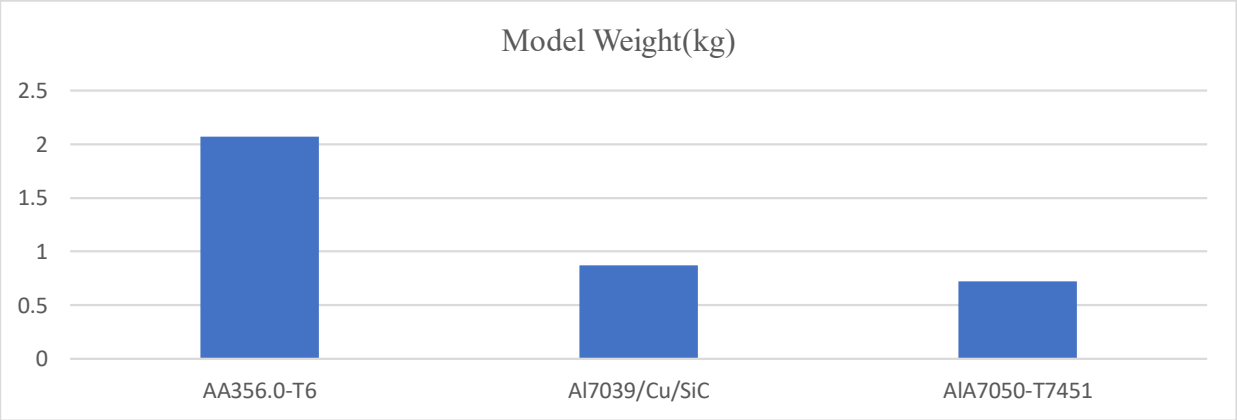

Figure 11 Weight Comparative Chart

4.3 Discussion of Results of Thermal Structural Analysis

This study investigated the thermal–structural performance of three aluminium-based materials — AA356.0-T6, Al7039/Cu/SiC, and Al7050-T7451 — for potential use in the connecting rod of a diesel engine. Using finite element analysis, each material was evaluated under combined thermal and mechanical loading, focusing on total deformation, von-Mises stress, equivalent elastic strain, and thermal stability.

The results revealed that Al7050-T7451 consistently outperformed the other materials in all evaluated parameters.

From Figures 3 – 10, and comparison Tables 5, Al7050-T7451 recorded the lowest total

deformation (2.9211mm), minimum von-Mises stress and (502.62 MPa), indicating exceptional stiffness, strength, and resistance to thermally induced stresses. These findings confirm the material's capacity to maintain structural and dimensional integrity under high-temperature and high-pressure conditions typical of diesel engine operation.

Comparatively, AA356.0-T6 and Al7039/Cu/SiC showed higher deformation of 27.719 mm and 29.778 mm respectively with stress values of over 11,000 MPa, suggesting lower thermal-mechanical efficiency. These results are consistent with earlier works by Zhao et al, 2019; (Singh and Patel, (2020), and Okoro and Adebayo (2021), who reported that Al7050-series alloys exhibit superior strength-to-weight ratios, high fatigue resistance, and excellent thermal stability compared to conventional cast aluminium alloys.

Based on the weight comparison in Table 6 and Figure 11, Al7050-T7451 has the lowest mass (0.7214 kg), followed by Al7039/Cu/SiC (0.8718 kg), while AA356.0-T6 is the heaviest (2.0716 kg). Al7050-T7451 is 65.17% lighter than AA356.0-T6 and 17.27% lighter than Al7039/Cu/SiC. Consequently, selecting Al7050-T7451 for the connecting rod is expected to enhance fuel efficiency (Singh and Patel, 2021), since vehicle weight and engine power are key factors influencing fuel consumption (Natural Resources Canada, 2011).

5.0 CONCLUSION

This study demonstrated that material selection has a decisive influence on the thermal–structural performance of connecting rods for diesel engine. Among the three aluminum-based materials investigated, Al7050-T7451 exhibited the best overall performance under coupled thermal and mechanical loading. It recorded the lowest total deformation (2.99211 mm) and minimum von-Mises stress (502.62 MPa), confirming its superior stiffness, strength, and resistance to thermally induced stresses. In contrast, AA356.0-T6 and Al7039/Cu/SiC showed comparatively higher deformation and stress levels, indicating reduced thermo-mechanical efficiency. Therefore, Al7050-T7451 is concluded to be the most suitable material for diesel engine connecting rods, with strong potential to improve durability, reliability, and operational efficiency.

Future studies should incorporate transient thermal–structural analysis to capture real engine operating cycles, including start-up, load variation, and shut-down conditions. Experimental validation using strain gauges and thermal measurements on a test engine is recommended to verify the numerical results. Further work may also consider fatigue life prediction, creep behaviour at elevated temperatures, and wear performance at the pin and crank interfaces. In addition, optimization studies focusing on geometry refinement and cost–performance trade-offs could enhance the practical applicability of Al7050-T7451 for large-scale engine manufacturing.

Symbols

Symbols	Interpretation
σ_{t1}	maximum principal or normal stress in a bi-axial stress system
σ_{t2}	minimum principal stresses in a bi-axial stress system
σ_{yt}	Yield point stress in tension as determined from simple tension test
σ_u	Ultimate stress
τ_{max}	Maximum shear stress in a bi-axial stress system
τ_{yt}	Shear stress at yield point as determined from simple tension test
ε_{max}	maximum principal (or normal) strain in a bi-axial stress system
ε	Strain at yield point as determined from simple tension test
l/m	Poisson's ratio
E	Young's modulus
F.S.	Factor of safety
σ_C	Compressive yield stress
W_B	Buckling load
I_{xx}	Moment of inertia of the section about X-axis
I_{yy}	Moment of inertia of the section about Y-axis
l	Length of the connecting rod
r	Radius of gyration
A	Cross-sectional area of the connecting rod
L	Equivalent length of the connecting rod
a	Rankine constant or =

Design Equations Parameters

Symbols	Interpretation
P_{max}	Maximum pressure of gas/effective pressure
D	Diameter of piston
A	Cross-section area of piston
m_R	Mass of reciprocating parts(mass of piston, gudgeon pin, etc) $+\frac{1}{3}$rd mass of connecting rod
ω	Angular speed of crank
φ	Angle of inclination of the connecting rod with the line of stroke
θ	Angle of inclination of the crank from top dead centre
r	Radius of crank
l	Length of connecting rod
n	Ratio of length of connecting rod to radius of crank = l/r
n_c	Number of cylinders
S	Stroke length(m)
N	Speed of the Engine

L	Equivalent length of the connecting rod, Both ends Hinged L=l , Both ends fixed L = l/2
Z	Section modulus
$\boldsymbol{d_c}$	Diameter of the crank pin in mm
$\boldsymbol{l_c}$	Length of the crank pin in mm, = $1.25d_c$ to $1.5d_c$($1.25\boldsymbol{d_c}$)
$\boldsymbol{P_{bc}}$	Allowable bearing pressure in N/mm^2 = 7 to 12.5 N/mm^2 (9.8N/mm^2)
$\boldsymbol{d_p}$	Diameter of the piston pin in mm
$\boldsymbol{l_p}$	Length of the piston pin in mm, = $1.5d_p$ to $2d_p$($\boldsymbol{1.75d_p}$)
$\boldsymbol{P_{bp}}$	Allowable bearing pressure for piston pin bush in N/mm^2 = 10.5 to 15 N/mm^2(15N/m^2)
$\boldsymbol{d_{cb}}$	Core diameter of the bolt in mm
$\boldsymbol{\sigma_t}$	Allowable tensile stress for the material of the bolts in MPa
$\boldsymbol{n_b}$	Number of bolts. Generally, two bolts are used
$\boldsymbol{d_b}$	Major Diameter of the Bolt
$\boldsymbol{t_c}$	Thickness of the big end cap
$\boldsymbol{\sigma_b}$	Bending stress
R	Number of rings
$\boldsymbol{P_R}$	Pressure of rings (0.025 to 0.04 N/mm2)
$\boldsymbol{\mu}$	Coefficient of friction (about 0.1).
$\boldsymbol{b_c}$	Width of the cap in mm. It is equal to the length of the crankpin or big end bearing (*lc*)

Abbreviations

FEM	Finite Element Method
FEA	Finite Element Analysis
IC	Internal Combustion
ICEs	Internal Combustion Engines
F.S.	Factor of Safety
UTM	Universal Test Machine
RPM	Revolution per Minute
MMCs	Metal matrix composites

ACKNOWLEDGEMENTS

First and foremost, I give all glory, honour, and adoration to the Almighty God, the source of wisdom, knowledge, and strength, for His endless grace and divine guidance throughout my academic journey. His favour and mercy have been my firm foundation, granting me perseverance and clarity to complete this dissertation successfully. Without His divine support, none of this would have been possible.

I sincerely appreciate the Dean of the Faculty of Engineering, Engr. Prof. John Wasiu, for his exemplary leadership, academic excellence, and commitment to quality education. My

profound gratitude also goes to the Head of the Department of Mechanical Engineering, Engr. Dr. S. Nihad Achekuogene, for his continuous support, motivation, and encouragement. I am deeply indebted to my Supervisor, Engr. Dr. F. Oamen Isaac, whose valuable guidance, patience, and constructive criticisms greatly shaped this research work. My appreciation equally extends to the academic and technical staff of the Department of Mechanical Engineering for their assistance, as well as my colleagues and classmates for their cooperation, friendship, and shared academic experiences.

Finally, I express my heartfelt gratitude to my beloved wife Mrs. B. Elizabeth Adediran, and lovely children in the family for their unconditional love, prayers, and moral support throughout this academic pursuit. Special thanks to my friends most especially late Pastor A. Ebenezer Ajayi, mentors, my bosses and colleagues at work for their understanding, encouragement, and inspiration during this journey. Their constant belief in my abilities and unwavering support has been instrumental in the successful completion of this dissertation.

REFERENCES

Adebayo, K. O., and Oyetunji, A. (2025). Effect of compositions weight fraction on surface roughness of Al7039/Cu/SiC MMCs: A central composite design approach. Bohrium Engineering Journal, 7(2), 115–123. https://www.bohrium.com/paper-details/effect-of-compositions-weight-fraction-on-surface-roughness-of-al7039-cu-sic-mmcs-a-central-composite-design-approach

Aerospace Metals. (2023). Aluminium 7050-T7451: Mechanical and physical property data. Retrieved from https://www.aerospacemetals.com/wp-content/uploads/2023/06/Aluminum-7050-T7451-7050-T73651.pdf

Anand. R, Raghukumar S., (2022) Design and Analysis of Connecting Rod Using Different Materials, Ijraset Journal for Research in Applied Science and Engineering Technology, DOI Link: https://doi.org/10.22214/ijraset.2022.42153

Andreas Ochsner, (2024) Collaborative research advancing engineering solutions for real-world challenges, pages 54-64.

ANSYS (2023). ANSYS Topology Optimization User's Guide. ANSYS, Inc
Arso W., Wan M.N.C, Ayob A.F.M., Mansor W.N.W., (2024), Failure Analysis of a Connecting Rod Bearing of a Diesel Engine Generator Set

Autodoc blog expert in auto parts-(online) 2023, Engine connecting rod: functions, problems, and failure symptoms

Avci, U., Turan, M. E., and Guler, S. (2017). A new approach to the production of partially graded and SiC-reinforced Al7039 alloy matrix composites. Composites Part B: Engineering, 131, 216–225. https://doi.org/10.1016/j.compositesb.2017.08.041

Azadi, M., Hashemi, R., and Nili-Ahmadabadi, M. (2013). Heat treatment effect on thermo-

mechanical fatigue and low-cycle fatigue behaviours of A356.0 and A356.0-T6 aluminium alloys. Materials Science and Engineering: A, 559, 161–168. https://doi.org/10.1016/j.msea.2012.08.045

Chirinda G., and Matope S.,(2020), The Lighter the Better: Weight Reduction in the Automotive Industry and its Impact on Fuel Consumption and Climate Change, Proceedings of the 2nd African International Conference on Industrial Engineering and Operations Management, Harare, Zimbabwe, December 7-10, 2020© IEOM Society International520

Fakharipasandi, M. (2023). A study of A356 aluminum alloy properties. Retrieved from https://www.researchgate.net/publication/371006769_A_Study_of_A356_Aluminum_Alloy_Properties

Gangarkar M., Prof. Prashant K., (2024), Optimization and Analysis of 4-Wheeler Connecting Rod for Weight Reduction and Performance Enhancement

Gautam A., Ajit K. P., Sharma P., Gautam A., Warudkar V., Bhagoria J. L., (2021), Failure Analysis of Alloy Steel Connecting Rod

Godara,S.S, BreniaV., Soni A. K., Shekhawat R. S., & Saxena K.K.,(2022), Design & analysis of connecting rod using ANSYS software, Materialstoday Proceedings, Volume 56, Part 4, April 2022, Pages 1896-1903, https://doi.org/10.1016/j.matpr.2021.11.166

Khurmi, R. and Gupta, J.K., (2005) A Textbook of Machine Design Text of Machine Design. Eurasia Publishing House (Pvt.) Ltd., New Delhi.]

Kumar, P., Singh, V., and Sharma, R. (2019). Thermo-mechanical analysis of high-strength aluminum alloys for automotive applications. Journal of Materials Engineering and Performance, 28(6), 3210–3221. https://doi.org/10.1007/s11665-019-04030-8

Lunn, K. F. (2024). Thermal and Electrical Conductivity of Aluminum Alloys: A Critical Review. Materials & Design, 225, 111–[pages].

Mohammed, S. A., Yusuf, H. M., and Lawal, A. (2017). Thermal stress analysis of AA356 aluminum alloy under cyclic loading conditions. International Journal of Mechanical Sciences, 134, 275–283.

Okoro, C. E., and Adebayo, O. M. (2021). Evaluation of Al7050 alloy for high-temperature engine components. Materials Today: Proceedings, 45, 1274–1281.

Okoro, C., and Adebayo, O. (2021). Mechanical characterization and performance evaluation of aluminum 7000 series alloys for automotive applications. International Journal of Engineering Research and Technology, 10(6), 1145–1152.

Orhadahwe, T. A. (2020). A Review on Primary Synthesis and Secondary Treatment of Aluminium-Matrix Composites. Advances in Engineering Materials, 22(3), 1-20.

Reddy, K. S. K., Kannan, M., and Karthikeyan, R. (2021). Evaluation of Mechanical and Thermal Properties of Aluminium-7475 Reinforced with Graphite and Fly Ash. E3S Web of Conferences, 85, 01186. https://doi.org/10.1051/e3sconf/20218501186

Singh, A., and Patel, K. R. (2020). Finite element modeling of Al7050 alloy for connecting rod applications under thermal loading. Engineering Failure Analysis, 114, 104613.

Singh, A., and Patel, R. (2021). Finite element assessment of lightweight connecting rods for improved fuel efficiency in diesel engines. Journal of Mechanical and Industrial Engineering Research, 9(2), 45–53

Smith Metal. (2023). Aluminium alloy 7050: Mechanical strength, stress corrosion resistance and toughness. Retrieved from https://www.smithmetal.com/pdf/aluminium/7xxx/7050.pdf

Teferi, F. T. (2025). Elevating Al7039 alloy performance through copper addition. Materials Research Express, 12(1), 016502. https://doi.org/10.1088/2053-1591/ada672

Teng, D., Lu, P., & Chen, Y. (2023). Response of mechanical properties of A356 alloy to different processing parameters. Materials Research Express, 10(5), 055004. https://doi.org/10.1088/2053-1591/acd250

Wang, J., Li, Q., and Zhao, Y. (2023). Microstructural characteristics and mechanical properties comparison of recycled 7050-T7451 alloy. Journal of Materials Research and Technology, 25, 448–459. https://doi.org/10.1016/j.jmrt.2023.05.041

Weichai Power Company Limited (2017), Operation and Maintenance Manual forWP10 Series Four-valve Diesel Engine (China IV, V), June 2017

Yildiz, A. R. and Yıldız, B. S, (2024) Advanced structural design of engineering components utilizing an artificial neural network and GNDO algorithm, Published/Copyright: November 27, 2024, https://www.degruyterbrill.com/document/doi/10.1515/mt-2024-0216/html

Yu Z., Xiaolei X., (2015) Fatigue Fracture of Truck Diesel Engine Connecting-Rods, April 2015, Journal of Failure Analysis and Prevention, 15(2) DOI: 10.1007/s11668-015-9934-7

Zhao, Y., Wang, Q., and Zhang, J. (2019). Fatigue Behavior of 7050-T7451 Aluminum Alloy. International Journal of Fatigue, 121, 278-287. DOI: 10.1016/j.ijfatigue.2018.12.014

Zhu X., Xu J., Liu Y., Cen B., Lu X., (2017), Failure analysis of a failed connecting rod cap and connecting bolts of a reciprocating compressor